Accepted Manuscript

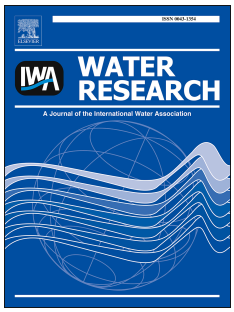

A generalised chemical precipitation modelling approach in wastewater treatment applied to calcite

Christian Kazadi Mbamba, Damien Batstone, Xavier Flores-Alsina, Stephan Tait

PII: S0043-1354(14)00706-4

DOI: 10.1016/j.watres.2014.10.011

Reference: WR 10927

To appear in: *Water Research*

Received Date: 14 June 2014

Revised Date: 17 September 2014

Accepted Date: 5 October 2014

Please cite this article as: Mbamba, C.K., Batstone, D., Flores-Alsina, X., Tait, S., A generalised chemical precipitation modelling approach in wastewater treatment applied to calcite, Water Research (2014), doi: 10.1016/j.watres.2014.10.011.

Highlights (for review)

- A general kinetic-based model for precipitation has been identified and validated.
- The model is first order in mineral state and *n*th order in supersaturation.
- The model is tolerant to a fast kinetic coefficient, but not a slow coefficient.
- The kinetic effect of temperature can be corrected with Arrhenius-relationships.
- This base model can be applied to multiple simultaneous precipitation reactions.

$$R_{cryst} = k_{cryst} X_{cryst} \sigma^{n}$$

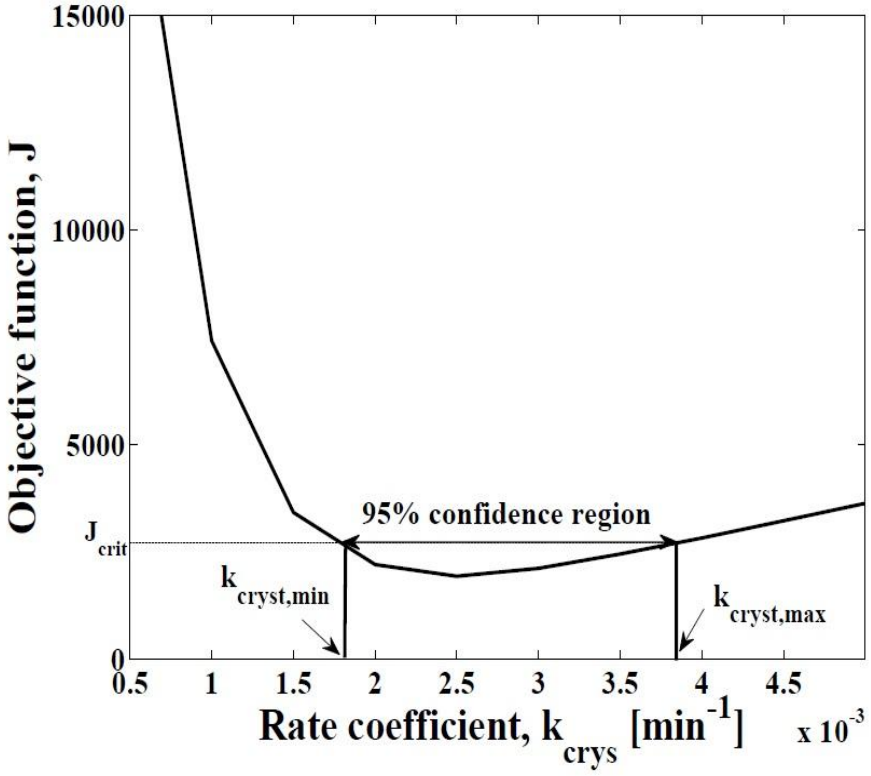

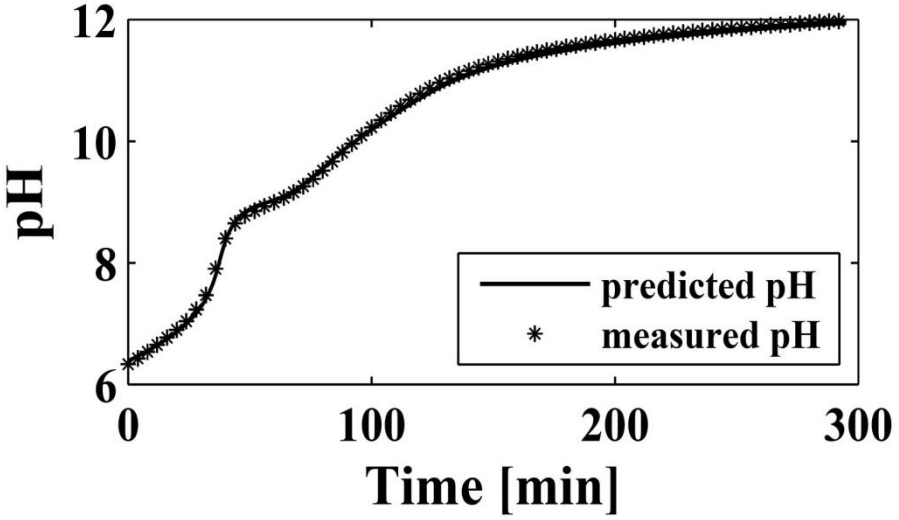

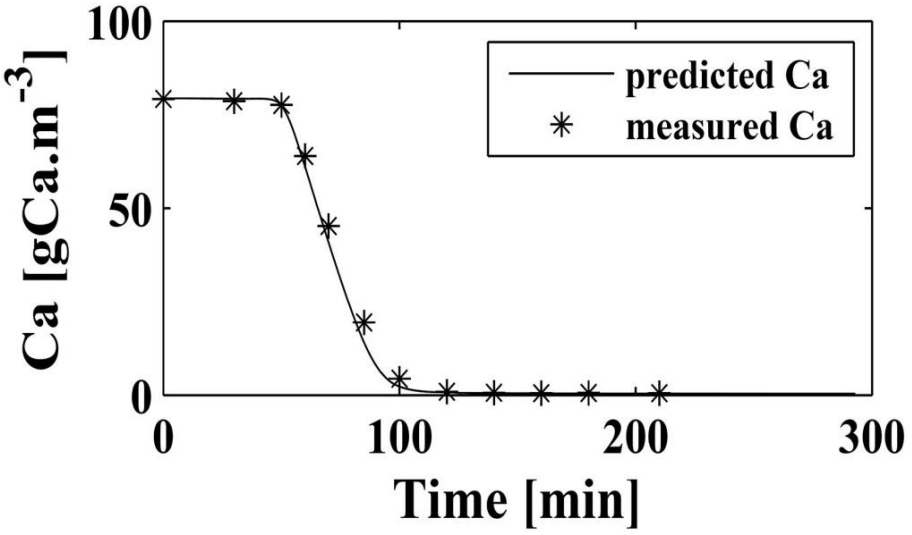

A generalised chemical precipitation modelling approach in wastewater treatment applied to calcite

Christian Kazadi Mbamba [a], Damien Batstone [a], Xavier Flores-Alsina [b], Stephan Tait [a]

[a] Advanced Water Management Centre, The University of Queensland, St Lucia, Brisbane, QLD 4072, Australia

[b] CAPEC-PROCESS, Department of Chemical and Biochemical Engineering, Technical University of Denmark, Building 229, DK-2800 Lyngby, Denmark.

ABSTRACT

Process simulation models used across the wastewater industry have inherent limitations due to over-simplistic descriptions of important physico-chemical reactions, especially for mineral solids precipitation. As part of the efforts towards a larger Generalized Physicochemical Modelling Framework, the present study aims to identify a broadly applicable precipitation modelling approach. The study uses two experimental platforms applied to calcite precipitating from synthetic aqueous solutions to identify and validate the model approach. Firstly, dynamic pH titration tests are performed to define the baseline model approach. Constant Composition Method (CCM) experiments are then used to examine influence of environmental factors on the baseline approach. Results show that the baseline model should include precipitation kinetics (not be quasi-equilibrium), should include a 1st order effect of the mineral particulate state (X_{cryst}) and, for calcite, have a 2nd order dependency (exponent n=2.05±0.29) on thermodynamic supersaturation (σ). Parameter analysis on the kinetic coefficient k_{cryst}, indicated that the model was more tolerant to a fast kinetic coefficient (k_{cryst}) and so, in general, it is recommended that a large k_{cryst} value be nominally selected where insufficient process data is available. Zero seed (self nucleating)

conditions could be effectively represented by including arbitrarily small amounts of mineral phase in the initial condition. Both of these aspects are important for wastewater modelling, where knowledge of kinetic coefficients, and precipitates present, are not usually known. The CCM experiments confirmed the baseline model, particularly the dependency on supersaturation. Temperature was also identified as an influential factor that should be corrected for via an Arrhenius-style correction of k_{cryst}. The influence of magnesium (a common and representative added impurity) on k_{cryst} was found to be significant but was considered an optional correction because of a lesser influence as compared to that of temperature. Other variables such as ionic strength and pH were adequately captured by the quasi-equilibrium description of the aqueous-phase and no further kinetic corrections were required. The baseline model is readily expandable to include other precipitation reactions. For simple representations, large values for k_{cryst} with n=2 (or n=2 or 3 for other minerals) should be selected without corrections to k_{cryst}, and, where accuracy is required (e.g., in mechanistic studies), machine estimation of k_{cryst} should be performed with robust process data and k_{cryst} should at least be corrected for temperature.

Keywords

Physico-chemical modelling, minerals precipitation, calcite, acid-base titration, equilibrium, kinetics

1. Introduction

In recent years, mathematical process modelling of wastewater processes has become an increasingly active field, with models being successfully used for research, process design, training, control and optimization of physical, chemical and biological processes. However,

to date the focus of model development has largely been on the biological reactions that occur during wastewater treatment (Henze et al., 2000; Batstone et al., 2002). Much less attention has been given to the many non-biological chemical reactions that occur in wastewater treatment, even though such reactions are essential to achieve effective treatment (Batstone et al., 2012). Process simulation models used across the industry currently have inherent limitations due to simplistic and situation-specific representations of important physico-chemical reactions (Batstone, 2009). A key neglected area is liquid-solid chemical precipitation modelling, due to its widespread occurrence in wastewater treatment processes (Doyle and Parsons, 2002; Chen et al., 2008; Batstone and Keller, 2003; van Langerak et al., 2000) and a general under-representation in existing standardised models (Batstone et al., 2012). Chemical precipitation is also particularly significant from a modelling perspective, because of heavy interactions with other physico-chemical reactions in the wastewater such as the weak acid-base system and ion complexation. A model containing chemical precipitation therefore automatically requires representation of other physico-chemical reactions, which is a key limitation of (for example) the ASM2d (Henze et al., 2000) which models precipitation without considering pH.

Several studies have used mathematical modelling to improve the understanding of chemical precipitation mechanisms in wastewater treatment (Barat et al., 2009; Maurer et al., 1999; Musvoto et al., 2000; Smith et al., 2008; Szabó et al., 2008; Tait et al., 2009; van Rensburg et al., 2003). Typically, unique modelling approaches have been applied to specific experimental datasets. Key differences between the various modelling approaches have included:

(a) an assumption that precipitation reactions are occurring at sufficiently rapid rates to be effectively at equilibrium (Smith et al., 2008; Hanhoun et al., 2011; Loewenthal et al., 1995;

Ohlinger et al., 1998; Scott et al., 1991; Wrigley et al., 1992) or instead treating them as kinetic reactions in the dynamic state equation set (Maurer et al., 1999; Musvoto et al., 2000; van Rensburg et al., 2003);

(b) accounting for the effect of the available mineral surface area on the overall rate of precipitation (Smith et al., 2008; Tait et al., 2009) or not (Musvoto et al., 2000); and

(c) assuming competitive or synergistic interactions are occurring between multiple chemical precipitation reactions occurring in parallel (Barat et al., 2011) or not (Musvoto et al., 2000).

In particular, more complex models that include multi-step precipitation with a broad range of controlling mechanisms tend to focus on specific applications, with generalised approaches being simplified to equilibrium and simple kinetics. To date, there has not been substantial experimental-based work focussed on systematically developing a general precipitation modelling approach. With increasing interest in correctly predicting precipitation such as struvite for phosphorus resource recovery (Rahaman et al., 2014; Galbraith et al. 2014), and with the rise in plant-wide model descriptions (Gernaey et al., 2011) to develop new control strategies that consider nutrient recovery, a generally applicable and robust model approach is required for both detailed mechanistic descriptions and broader engineering analysis.

In this paper, a baseline precipitation model approach is developed in the context of calcite precipitation and further analysis then focuses on clarifying key environmental factors that influence precipitation modelling. The model approach is intended to form part of a larger Generalized Physicochemical Modelling Framework (Batstone et al., 2012) but is also intended for use across a wider range of wastewater applications. The paper is structured to first present the baseline precipitation model validated via dynamic pH titration tests, after which Constant Composition Method (CCM) experiments and robust statistics are used to examine the influence of environmental factors.

2. Materials and methods

Experiments investigated the precipitation of calcite (a crystalline form of calcium carbonate) from synthetic aqueous solutions. Two experimental platforms were used, namely, dynamic pH titration tests with precipitation, and the Constant Composition Method (CCM). Titration was used to identify the baseline model approach across a range of pH values, and CCM tests investigated the influence of environmental factors on the baseline model approach. In continuous pH titration the aqueous solution is titrated from a low pH to a high pH with precipitation or dissolution of minerals occurring along the way. The Constant Composition Method maintains a constant chemical composition while precipitation occurs, by continuously adding a titrant to replenish soluble ingredients that are being sequestered by the precipitating mineral (Tomson and Nancollas 1978). The rate of precipitation for a CCM test can then be directly quantified from the amount of titrant added over time.

2.1 Materials

Analytical reagent-grade chemicals and de-ionised water were used in all cases. Metastable (no spontaneous nucleation) supersaturated test solutions were prepared by adding an aqueous solution of calcium chloride ($CaCl_2$) at a known concentration, drop-wise over 20-30 minutes, to an aqueous solution of sodium bicarbonate ($NaHCO_3$) at a known concentration. The ionic strength of test solutions was altered with dissolved potassium chloride. The inorganic carbon reagent solution was always prepared fresh. Synthetic calcite seed crystals were prepared similarly in a 50:50 mix of $CaCl_2$ and sodium carbonate (Na_2CO_3) solutions at 25^{o}C, but at a much higher dissolved calcium carbonate concentration of 0.4 M to induce

126 spontaneous nucleation. The addition of $CaCl_2$ was much slower for the seed preparation
127 (dropwise over about 2-3 hours). Freshly precipitated seed crystals were aged for 2 days in
128 their mother liquor and were subsequently extensively washed with distilled water. The
129 washed seed crystals were aged for at least 3 weeks in a 0.02 M aqueous solution of
130 $NaHCO_3$, then filtered and again washed with distilled water. Adhering water was displaced
131 with absolute ethanol which in-turn was evaporated off at 18-20°C in a desiccator to
132 minimize re-exposure to moisture. The crystals were examined using X-ray diffraction
133 analysis as per the method below and only peaks for calcite were detected. Specific surface
134 area and crystal morphology were examined by nitrogen adsorption and scanning electron
135 microscopy, respectively, as described below.
136
137 ***2.2 Apparatus***
138
139 The dynamic titration experiments used an auto-titrator (T50, Mettler-Toledo, Greifensee,
140 Switzerland) with a pH sensor (Model DGi115-SC, Mettler-Toledo, Greifensee,
141 Switzerland). The titrator was equipped with a 10 mL burette to add titrant to the test
142 solutions. Titration vessels used were (a) 100 mL beakers, with working volumes of 75 mL or
143 b) a 1 L stirred glass crystallizer. During a titration, the test sample to which titrant was added
144 was stirred with a 25 mm teflon-coated magnetic bar stirrer at 300 rpm. The volume of each
145 titrant added, the pH and the temperature were recorded over time through a LabX Light
146 Titration Software interface (Mettler-Toledo, Greifensee, Switzerland).
147
148 The CCM experiments used a crystallizer (See schematic in Supporting Information) which
149 was a 1.0 L (working volume = 900 mL) Pyrex glass vessel with a glass heating/cooling
150 jacket and a sealed lid with crimp-sealed ports for sensors to minimize atmospheric gas-

exchange. The crystallizer, positioned over a magnetic stirrer plate, was stirred with a 40 mm teflon-coated magnetic bar stirrer at 350 rpm. Water was circulated from a temperature-controlled water bath through the jacket to maintain the temperature inside the crystallizer to within ±0.5°C. A change in the continuously measured pH (S900C, Sensorex, Garden Grove, USA) triggered the simultaneous addition of two titrants by high-accuracy self-priming micropumps (120SP, 130SP, Bio-Chem Valve, New Jersey, USA), which replaced the dissolved calcium and inorganic carbon and maintained a constant pH (to within 0.1%) and aqueous phase composition (to within 1.5% of the set concentrations). The volume of each titrant added was recorded over time through a LABVIEW VI Software interface (v. 11.0, National Instruments, Austin, USA) via a multifunction data acquisition card (iUSBDAQ U120816, Hytek Automation, Ontario, Canada). Calcium ion activity was also monitored with an ion selective electrode (Model 361-75, Sentek, Essex, UK) and was recorded.

2.3 Experimental protocol

For the dynamic titration tests, the pH of a 1 L aliquot of test solution with known composition (actual volume known accurately) was adjusted to a desired initial value with concentrated sodium hydroxide (NaOH) or hydrochloric acid (HCl) solution, with the amount of added acid or caustic recorded. A 2M aqueous solution of NaOH (5-10 mL total) was then quantitatively added at a predetermined fixed rate and pH was continuously measured. For each experiment, pH and the rate and volume of titrant added were continuously recorded with the control software as was the volume of the original test solution. For chemical analysis, 1.1 mL samples of the titration vessel contents were collected at specified time intervals, immediately filtered through 0.2 μm cut-off syringe filters (PES), diluted with deionized water to prevent post-precipitation and stored at 4^{o}C until analysis by Inductively

Coupled Plasma Optical Emission Spectroscopy (ICP-OES) and a Total Carbon Analyser as detailed below. The experimental conditions were as follows:

a) 2.6M NaOH added at a rate of 2.5×10^{-5} mL.min^{-1} to a synthetic aqueous solution with 4.95mM sodium bicarbonate ($NaHCO_3$) and 1.96mM calcium chloride ($CaCl_2$) with initial pH decreased by adding a small quantity of concentrated HCl.
b) 2.35M NaOH added at a rate of 2.5×10^{-5} mL.min^{-1} to a synthetic aqueous solution with 4.86mM $NaHCO_3$ and 1.95mM $CaCl_2$ (initial pH was also decreased with concentrated HCl) and 50 mg.L^{-1} of calcite seed added when the saturation index (*SI*) value was estimated to be near zero (See below).
c) 2.6M NaOH added at a rate of 2.5×10^{-5} mL.min^{-1} to a synthetic aqueous solution with 4.87mM $NaHCO_3$ and 1.98mM $CaCl_2$ (initial pH was decreased with concentrated HCl) and 200 mg.L^{-1} of calcite seed material when the *SI* value was estimated to be near zero (See below).

For the CCM tests, metastable test solutions were added to the crystallizer and while stirring, the initial pH was adjusted by drop-wise addition of 1M NaOH or HCl as required. Once the measured pH was stable, precipitation was initiated by adding a weighed amount of calcite seed crystals. Usually, this seed addition immediately triggered titrant dosing. Separate sets of experiments were performed to assess the effect of various environmental factors (See Table 1 for test conditions). Measured calcite precipitation rate (R_{calcite}, moles.L^{-1}.min^{-1}) for each CCM experiment was determined as follows:

$$R_{\text{calcite}} = C_{\text{eff}} q_{\text{t}} \quad (1)$$

where q_{t} is the titrant flow rate (L.min^{-1}) and C_{eff} is the equivalent number of moles precipitated per litre of added titrant per L of reactor vessel (moles.L^{-1}.L^{-1}). Values of q_{t} were determined by linear regression fits of the cumulative volume of titrant added over time.

2.4 Analytical techniques

X-ray diffraction analysis (Bruker D8, Bruker, Massachusetts, USA) of the seed crystals, only detected peaks for calcite and had a clear background. The specific surface area of the seed crystals was measured by nitrogen adsorption (Tristar II 3020, Micromeritics, Norcross, GA) and is given in Table 1. Seed crystal morphology was examined with scanning electron microscopy (JEOL 2100, JEOL Ltd, Tokyo, Japan) and was found to resemble the typical morphology of calcite with reasonably uniform particle size.

The major elements (Ca, Na) in the synthetic aqueous solution were analysed with ICP-OES (Perkin Elmer Optima 7300DV, Waltham, MA, USA). Total Inorganic Carbon (TIC) concentrations were quantified using a Total Carbon Analyser (Shimadzu TOC-L CSH Total Organic Carbon Analyser, Kyoto, Japan).

2.5 Data and model analysis

A reduced form of the draft generalised physicochemical model (See Supplementary Material) was used with states that were not being utilised, deactivated in the code for the sake of speed and simplicity. The baseline precipitation model approach applies an algebraic equation set for fast aqueous-phase reactions such as weak acid-base and ion pairing, and simple kinetics for mineral precipitation reactions.

2.5.1 Aqueous-phase reactions: Algebraic equation set

226 Weak acid-base reactions and ion pairing were mathematically described with a set of non-
227 linear algebraic equations as is commonly done in geochemical reference models (Allison et
228 al., 1991; Parkhurst and Appelo, 1999). The equation set included one law of mass-action
229 (see Eq. (2)) for each aqueous phase reaction and a number of molar contribution balances
230 (see Eq. (4)) to satisfy the required degrees of freedom for the calculation. In general form,
231 the mass action laws were:

$$K_{\mathrm{i}} = \prod_{\mathrm{j}=1}^{N} S_{(\mathrm{j})}^{\nu_{\mathrm{ij}}} \qquad i = 1, 2 \ldots, N \tag{2}$$

232 where K_{i} is the equilibrium constant for aqueous phase reaction i, $\nu_{\mathrm{i,j}}$ is the stoichiometric
233 coefficient of the reactant or product j for aqueous phase reaction i, and $S_{(\mathrm{j})}$ is soluble
234 concentrations expressed in terms of chemical activities, applied as corrections due to
235 deviations from ideality. Chemical activities are equal to the actual physical soluble
236 concentrations S_{j} multiplied by a correction factor γ_{j} as follows (Eq. (3)):

$$S_{(\mathrm{j})} = \gamma_{\mathrm{j}} S_{\mathrm{j}} \tag{3}$$

238 where $S_{(\mathrm{j})}$ is the chemical activity and γ_{j} is activity coefficient describing how interactions
239 among charged ions influence chemical behaviour. The extent of correction for non-ideal
240 behavior depends on the ionic strength of the wastewater, with increasing corrections
241 required for a higher ionic strength. In this work, the Davies approximation to activity
242 coefficients was used with temperature correction. Equilibrium constants (K_{i}) were also
243 adjusted for temperature using the constant-enthalpy form of the van't Hoff equation.
244
245 In general form, the molar contribution balances were:

$$S_{\mathrm{i,tot}} = \sum_{\mathrm{i}=1}^{\mathrm{N}} S_{\mathrm{i}} \tag{4}$$

where $S_{i,tot}$ is the total measurable concentration of an aqueous phase ingredient which is the sum contribution of that ingredient in various chemical forms in the aqueous phase.

In this work, a reactive proton balance (a molar contribution balance) was used for pH calculations as done by others (Serralta et al, 2004). The reactive proton balance (TotH) approach is noted to be fully compatible with the alternative charge balance/electroneutrality approach. Indeed, a charge balance model was also run and the results were identical to that of the TotH model. As is commonly done, the mass action laws were substituted into the molar contribution balances until all the remaining substituted equations were linearly independent (the most reduced form of the algebraic equation set). The Tableau method (Morel and Morgan, 1972) was used to guide this substitution of equations which reduced the number of equilibrium variables from 25 (H^+, Na^+, K^+, Cl^-, CO_3^{-2}, Ca^{2+}, Mg^{2+}, $CaCl^+$, $CaCO_3$, $CaHCO_3^+$, $CaOH^+$, H_2CO_3, HCO_3^-, KCl, KOH, $Mg_2CO_3^{+2}$, MgCl+, $MgCO_3$, $MgHCO_3^+$, MgOH+, NaCl, $NaCO_3^-$, $NaHCO_3$, NaOH, OH^-) down to seven (H^+, Na^+, K^+, Cl^-, CO_3^{-2}, Ca^{2+}, Mg^{2+}). The former are commonly called chemical species and the latter are called chemical components. The chemical species were calculated from the mass action laws and the solved chemical components.

The implicit algebraic equation set was iteratively solved by the Newton-Raphson (NR) method as follows:

$$Z_{i+1}=Z_i-\nabla G(Z_i)^{-1}\,G(Z_i) \tag{5}$$

where Z_i is the vector of equilibrium variables ($z_{1,i}$, …, $x_{n,i}$) obtained from the previous iteration step i, $G(Z_i)$ is a vector containing the values of the set of implicit algebraic equations ($g_1(z_1, \ldots, z_n)$, …, $g_n(z_1,\ldots, z_n)$) which has to be zero in order to satisfy equilibrium and $\nabla G(Z_i)$ is the function gradient for step i. The iteration was repeated as long as the elements

of the error function are larger than a predefined value, which in this case was set to 10^{-12}. A reduced analytical 1-D gradient ($\nabla G = [{}^{\partial g_1}/_{\partial z_1} \ldots {}^{\partial g_n}/_{\partial z_n}]$) considering only the identity elements was used in this case due to its convergent nature and to increase speed, but the full gradient could also be used for a more complex system. The aqueous phase model results were verified against Visual MINTEQ (Version 3.0, Royal Institute of Technology (KTH)) and thermodynamic parameters were also sourced from the Visual MINTEQ database. The set of algebraic equations were solved for each time step with precipitation implemented as rate equations (ordinary differential equations). The method used solves the differential equations separately with an ODE solver in SIMULINK, and then iterates at each time step the accompanying nonlinear algebraic system using an iterative solver (Newton-Raphson method). As a result, the pH and aqueous species concentration were calculated as a function of time through a series of differential algebraic equations (DAEs).

The species and components were also used to determine precipitation or dissolution, by calculating the well-known indicator, the Saturation Index (*SI* value):

$$SI = \log_{10}\left(\frac{S_{(\mathrm{Ca^{2+}})} \times S_{(\mathrm{CO_3^{2-}})}}{K_{\mathrm{sp,calcite}}}\right) \quad (6)$$

where $S_{(Ca+2)}$ and $S_{(CO3-2)}$ are the chemical activities of calcium and carbonate ions in the aqueous phase and the solubility product constant for pure calcite ($K_{SP,calcite}$) was taken to be $10^{-8.48}$ at 25°C (Nordstrom et al., 1990; Plummer and Busenberg, 1982). For a given aqueous phase, three conditions exist:

- $SI < 0$, the aqueous phase is undersaturated and a mineral solid phase can dissolve into the aqueous phase;
- $SI = 0$, the aqueous phase is saturated or at equilibrium; or

- $SI > 0$, the aqueous phase is supersaturated or oversaturated with respect to the mineral and chemical precipitation can occur.

In general, the *SI* value can help a model developer to select relevant mineral precipitation reactions for inclusion in the model (if $SI > 0$, or if $SI < 0$ and mineral phase is present).

2.5.2 Precipitation: Simple kinetics

Calcium carbonate precipitation was modelled with three dynamic state equations for total dissolved calcium, total dissolved inorganic carbon and the particulate calcite mineral phase. The baseline model proposed in this paper, used a semi-empirical kinetic rate law (Nielsen and Toft 1984, Stumm and Morgan 1996):

$$R_{\text{calcite}} = k_{\text{cryst}} X_{\text{CaCO}_3} \sigma^n \qquad \text{with } n=2 \tag{7}$$

where R_{calcite} is the calcite precipitation rate (moles.L^{-1}.min^{-1}), k_{cryst} is an empirical kinetic rate coefficient (min^{-1}), X_{CaCO_3}(moles.L^{-1}) is the concentration of calcium carbonate precipitate at any time *t* (a dynamic state variable) (similar to the approach of (Wiechers et al., 1975)) and n is the order of the precipitation reaction with respect to supersaturation, σ, calculated as follows (Nielsen, 1984):

$$\sigma = \left(\frac{S_{(\text{Ca}^{2+})} \times S_{(\text{CO}_3^{2-})}}{K_{\text{sp,calcite}}} \right)^{\frac{1}{2}} - 1 \tag{8}$$

A non-zero initial condition of X_{CaCO_3} of 1×10^{-6} M (which is 0.1 mg.L^{-1}) was used to model the dynamic titration experiment that had no seed crystals added (self-nucleating).

The gaseous species carbon dioxide (CO_2) is not considered in this model (only dissolved $H_2CO_3^*$), because prevailing low concentrations of inorganic carbon and pH adjustment with sodium hydroxide (rather than by aeration), caused little to no stripping of CO_2 during the

experiment. In cases where CO_2 mass transfer would be important, a model could readily include the gas stripping or dissolution as a kinetic or quasi-equilibrium process as per Batstone et al. (2002).

2.5.2 Model analysis

The only adjustable parameter in the baseline model (Eq. (7)) was k_{cryst}, because the algebraic equation set was entirely resolved by thermodynamics with no adjustable parameters. The best fit value of k_{cryst} was estimated by simultaneously fitting pH titration data from three separate experiments with very different experimental conditions, using a non-linear parameter estimation technique, *lsqcurvefit*, in MATLAB. Calcium concentration was selected as the fitted output and the residual sum of squares was selected as the objective function (*J=RSS*). The model was implemented in MATLAB S-Function/SIMULINK (Version 8.1, MathWorks Inc.) and the complete model code is also included in the Supplementary Material. Errors in parameters were generally estimated by two-tailed *t*-tests based on linear estimates of standard error, but where necessary, true confidence intervals were estimated based on an F-test in *J* as follows:

$$J_{\text{crit}} = J_{\text{opt}}\left(1 + \frac{p}{n_{\text{data}} - p}\right) F_{0.95,p,n_{\text{data}}-p} \quad (9)$$

where J_{crit} is the 95% confidence objective function (where $p=p_{95}$), p is the number of parameters (1), n_{data} is the number of data points, and $F_{0.95,p,ndata-p}$ is the cumulative F distribution value.

Further model analysis tested the importance of various optional corrections to k_{cryst} for the influence of environmental factors, and sought to validate the linear dependency of precipitation rate on X_{CaCO_3} and the exponent n=2 in Eq. (7). For this purpose, an Analysis of

343 Variance (ANOVA) first identified significant singular and interaction effects of
344 environmental factors on calcite precipitation rates measured in the CCM experiments. Other
345 CCM tests (Lin and Singer, 2005) typically examine normalized precipitation rates
346 (precipitation rate divided by mineral surface area) instead of raw precipitation rates (not
347 normalized) as determined by Eq. (1), but in the present study, raw precipitation rates were
348 preferred as a more applicable approach. ANOVA was carried out with the software package
349 R (Version 3.0.1, 2013-05-16, The R Foundation for Statistical Computing) with a
350 significance threshold of 5%. Non-linear regression analysis was then performed with the
351 *nlinfit* function in MATLAB to assess the significant environmental effects, either as kinetic
352 corrections to k_{cryst} or by parameter estimating the exponent n on supersaturation. The
353 regression analysis also clarified the effect of X_{CaCO_3} in Eq. (7) by determining a power-law
354 dependency (y) of the precipitation rates on X_{CaCO_3} as follows:

355 $$R_{\text{calcite,measured}} = k_{\text{cryst}}\left(X_{CaCO_3}\right)^{y}\sigma^{n} \qquad k_{\text{cryst}}, y \text{ and } n = \text{estimated parameters} \quad (10)$$

356

357 The correction for added magnesium impurity was approximated with an adsorption style
358 relationship as follows:

$$k_{\text{cryst,corrected,Mg}} = k_{\text{cryst}} \times \left(1 - \frac{K_{\text{ads}} \times S_{Mg^{2+}}}{K_{\text{ads}} \times S_{Mg^{2+}} + 1}\right) \quad (11)$$

359 where S_{Mg+2} is the free dissolved magnesium ion concentration and K_{ads} is an empirical
360 adsorption coefficient (L.mole^{-1}). The form of Eq. (11) was selected because magnesium is
361 said to adsorb and block growth sites on the calcite crystal lattice instead of calcium ions due
362 to chemical similarity between calcium and magnesium (Reddy and Wang, 1980; Lin and
363 Singer, 2009; Chen et al,. 2006; (Ferguson and McCarty, 1971)). The kinetic effect of
364 temperature (in degrees Kelvin) was corrected for with the correction form of the Arrhenius-
365 style relationship:

$$k_{\text{cryst,corrected,T}} = k_{\text{cryst,25}} \times e^{-\frac{E_a}{R}\left(\frac{1}{T}-\frac{1}{298}\right)} \quad (12)$$

where $k_{cryst,25}$ is the reference value of k_{cryst} at 25°C (298K), R is the ideal gas constant (8.314×10^{-3} kJ.mol^{-1}.K^{-1}) and E_a is an empirical activation energy (kJ.mol^{-1}).

3. Experimental results

3.1 Dynamic titration experiments

Three titration experiments under very different conditions (200 mg.L^{-1} added seed, 50 mg.L^{-1} added seed, 0 mg.L^{-1} added seed) were fitted with the baseline model of Eq. (7), giving an estimated value for k_{cryst} of 0.0025±0.0004 min^{-1} (±linear estimate of 95% confidence interval). Fig. 1 presents the fit together with the experimental data and shows that the baseline model fit all three experiments qualitatively well. The model fit of the experiment with 0 mg.L^{-1} added seed was found to be insensitive to nominated X_{CaCO_3} concentrations below 1×10^{-5} M.

The objective function J (residual sum of squares) is presented in Fig. 2 and shows that the true 95% confidence region for k_{cryst} was 0.0018-0.0038 min^{-1} ($J_{crit,95}$= 2764.8). Fig. 2 also shows strong asymmetry which suggests that the model is more tolerant of high values of k_{cryst} as opposed to low values of k_{cryst} and thus a quasi-equilibrium approach (arbitrary high value of k_{cryst}) may be a valid approach where insufficient process data exists (see Discussion). However, Fig. 3 presents simulated and calculated saturation index values (*SI*), and clearly shows that *SI* values were never zero during precipitation between 30-200 minutes (never at equilibrium). These results suggest that the precipitation was still

kinetically limited, albeit that the SI values were generally less positive for a larger amount of added seed (see Discussion).

3.2 Constant composition experiments

The constant composition (CCM) experiments sought to clarify the influence of environmental factors on the baseline model approach of Eq. (7). Fig. 4 presents typical results from CCM experiments and shows that the rate of titrant addition ($q_t = dV/dt$) was stable. This translates to a single constant value of $R_{calcite}$ measured for each experiment. Table 2 presents results for the Analysis of Variance which indicated a very strong influence of supersaturation, σ (P<0.0001), in agreement with the baseline modelling approach of Eq. (7). Water temperature (T) was also found to have strong influence (P<0.001). The effect of added magnesium impurity (S_{Mg+2}) was noted to be significant (P<0.05), but was much weaker than the influence of T. Higher order effects of magnesium, temperature and supersaturation was also found to be statistically significant (Table 2). However, the impact of these higher order effects on k_{cryst} is expected to be too small to justify a more complex model that accounts for these influences. The effects of ionic strength (μ) and pH were found to be not significant (Table 2, P>0.05) or have low effect, and indicates that their influence on kinetics has been appropriately resolved via calculations of supersaturation (σ) with the algebraic equation set.

To show the performance of the baseline model approach of Eq. (7) with and without optional corrections for magnesium and temperature, Fig. 5 presents a comparison of measured precipitation rates from the CCM Test 1 (Table 1) vs. fitted precipitation rates via the non-linear regression analysis. Fig. 5A presents the baseline model fits of Eq. (7) without

optional corrections, Fig. 5B presents the baseline model fits with k_{cryst} corrected only for temperature and Fig. 5C presents the baseline model fits with k_{cryst} corrected for both magnesium and temperature. In general, the model fit appears to be qualitatively good only if a temperature correction is applied with Eq. (12) (then R^2 is >0.9). The R^2 values in Figs. 5B and C show that corrections for the influence of magnesium on k_{cryst} (Eq. (11)) and temperature on k_{cryst} (Eq. (12)) were significant and appropriate.

A regression analysis was also used to confirm the effects of X_{CaCO_3} and supersaturation in Eq. (7), by determining power-law exponents y (Eq. (10)) and n (Eqs. (7) and (10)). This analysis identified that y=1 (linear dependence in crystal mass, X_{CaCO_3}) and n=2 (2nd order dependence in supersaturation, σ), in support of Eq. (7) (see below). Table 3 presents the estimated values for y and n together with fitting parameters for Eqs. (11) and (12), namely, K_{ads}, $k_{cryst,25}$ and E_a. Precipitation rates were found to generally increase with increasing supersaturation and increasing added seed concentration ($X_{CaCO_3}(0)$), and the value of k_{cryst} and precipitation rates generally increased with increasing temperature and decreased with increasing magnesium concentration. Most importantly, the exponent y on X_{CaCO_3} was found to be 0.96±0.2 (given ±95% confidence interval), which indicates a linear relationship as per Eq. (7), and the exponent n was found to be 2.05(±0.29) for experiments with added magnesium and 1.3-1.6(±0.2) for experiments without added magnesium.

4. Discussion

4.1 Baseline modelling approach

438 A number of environmental factors can influence minerals precipitation in a wastewater.
439 However, results in this paper suggest that a model may only need to consider a limited
440 number of key effects, including supersaturation, the amount of mineral phase present in the
441 wastewater and wastewater temperature (Table 2, Table 3). The findings lead to the simple
442 and robust baseline approach in Eq. (7), with a linear dependency on the mineral solid state
443 X_{CaCO_3}, a 2nd order dependency on supersaturation and a single adjustable parameter k_{cryst}.
444 This approach has the major advantage of not requiring detailed analysis of mineral surface
445 area present in the wastewater, while still being able to model induction where very low seed
446 concentrations exist. This is important because the amount of mineral surface area is one of
447 the most influential factors for precipitation reactions (Wiechers et al., 1975). Larger amounts
448 of mineral phase forces the precipitation or dissolving of a mineral in a wastewater towards
449 equilibrium, and equilibrium is achieved much faster. This is seen in Fig. 3, where an
450 experiment with a larger amount of added calcite seed had lower *SI* values between 30 and
451 100 minutes, because of more rapid precipitation. Solids precipitation is driven by the
452 mineral surface area available in the wastewater. However, it is difficult or impossible to
453 reliably estimate the amount of mineral surface area in a wastewater. Consequently, a lumped
454 growth rate parameter has been common with no separate treatment of mineral phase or
455 mineral surface area (Batstone et al., 2002; van Langerak et al., 2000; Musvoto et al., 2000).
456 The results of the dynamic titration experiments (Fig. 1) indicated that the baseline model
457 approach of Eq. (7) with X_{CaCO_3} provided reasonable flexibility and model prediction
458 capability. The constant composition experiments provided further support of this baseline
459 model approach by validating the linear dependency of precipitation rates on X_{CaCO_3} (Table
460 3) and by confirming the second-order dependency of precipitation rate on supersaturation σ
461 (Table 3).
462

Parameter estimation (Fig. 2) indicated that the baseline modelling approach was tolerant to quasi-equilibrium (high value of k_{cryst}) but not to slow kinetics (low value of k_{cryst}), so the default approach should adopt a high value for k_{cryst}. This is shown in Fig. 2 which has strong asymmetry with a sharper increase in the value of the objective function *J* for lower values of k_{cryst} (below 0.0018 min^{-1}) and a very gradual increase in the value of *J* at higher values of k_{cryst} (above 0.0038 min^{-1}). Having some minimal quantities of mineral seed in a system is not a problem, since the parameter fit was relatively insensitive to seed concentration below 1 $mg.L^{-1}$ and hence this can be used as a default initial condition where the amount of mineral phase present is nil or unknown but small. While the model was more tolerant to high values of k_{cryst} (indicating that it is equilibrium-limited), it is noted from Fig. 3 and a survey of the wastewater modelling literature (Barat et al., 2011; Joss et al., 2011; van Langerak et al., 1999) that *SI* values for calcite/aragonite are either significantly positive or negative in wastewater, so precipitation or dissolution have not usually attained strict equilibrium, even within the timeframe of biological processes. Accordingly, it is suggested that, although the model is more tolerant to high values of k_{cryst}, it remains kinetically limited as indicated by the non-zero *SI* values (Fig. 3).

Eq. (7) is a general approach to simulate precipitation processes from a reaction-based mechanistic standpoint and is designed to be easily coupled with biological models. Such a kinetic-based model allows chemical precipitation reactions to occur with each model timestep to achieve a resulting solution composition which may still have a significant supersaturation state. Although the validation is based on calcite precipitation, the model structure can be easily expanded to include precipitation of many other minerals of interest in wastewater treatment, with appropriate selection of *n*. As the approach is general, it is possible to implement the precipitation model to calculate the pH for precipitating systems

488 and to simulate precipitation in whole-of-plant models. In full-scale facilities, it is expected
489 that mineral precipitates would be continuously recycled, such that the linkage of rate to
490 precipitate is implicitly included. The presence of and recycling of heterogeneous surfaces
491 (e.g. grit or particulate organics) in wastewater can and probably does induce heterogeneous
492 nucleation and thus minerals precipitation. Nevertheless, it is expected that this would not
493 greatly influence the model approach proposed in Eq. (7), for two reasons; (1) nucleation
494 (whether homogeneous, or more likely heterogeneous) is allowed for in Eq. (7) by seed
495 crystal for each relevant mineral, which accounts for induction kinetics and (2) heterogeneous
496 nucleation is likely to speed up overall precipitation, which is consistent with the default
497 selection of a fast k_{cryst} in cases where kinetics cannot be fully defined by available data.
498
499 Minerals that can precipitate in a wastewater treatment plant include phosphate minerals,
500 carbonate minerals, magnesium ammonium phosphate (struvite), sulfide minerals (at
501 anaerobic conditions) and hydroxides of aluminium and iron (Batstone et al. 2012). Not all of
502 these precipitating reactions take place at all wastewater conditions. Some of these minerals,
503 in particular calcium carbonate and calcium phosphate, are capable of crystallizing out of
504 solution in a variety of different mineral forms (crystalline vs. amorphous, and/or various
505 crystalline polymorphs). It is suggested that the kinetics of transformation from a less to more
506 stable mineral phase can be described by the baseline model approach proposed in Eq. (7), by
507 implementing both polymorphs/phases as parallel competitive reactions with dedicated rate
508 laws. The less stable polymorph/phase can then initially form and ultimately redissolve (via
509 the use of a reversible precipitation reaction) while the more stable polymorph/phase forms
510 over long process times. As precipitation mechanisms in wastewater become clearer (e.g.,
511 polymorphs) or where kinetic performance is more important, the proposed model can be

512 readily expanded with additional rate processes (e.g., stable polymorphs in parallel with a
513 slow k_{cryst} and high K_{sp}).
514
515 *4.2 Optional model corrections*
516
517 The model analysis using data from the constant composition experiments (Table 2)
518 highlighted wastewater temperature as an important environmental factor and a need for
519 temperature corrections of k_{cryst}. This is also shown in Fig. 5 where the model fit is only
520 deemed statistically acceptable (R^2>0.9) when temperature correction of k_{cryst} was applied.
521 Water temperature was observed to be a highly influential environmental factor (Table 2)
522 with the rate of precipitation approximately tripling with a 10°C increase in temperature. A
523 relevant temperature range for wastewater treatment might be 10-50°C, particularly where
524 temperature is artificially manipulated (e.g., in digesters and stripping). Both to account for
525 seasonality and for artificial temperature variations in a plant-wide model, temperature
526 correction of kinetics should be applied and an Arrhenius-style kinetic correction of k_{cryst} is
527 suggested (Eq. (11)). There is still a general lack of activation energy (E_a) values for all the
528 relevant minerals in wastewater (Batstone et al., 2012), although some values are available
529 for relevant minerals (Harmandas and Koutsoukos, 1996; Boskey and Posner, 1973; Inskeep
530 and Silvertooth, 1988). An estimate of E_a for calcite from the present work ($E_a \approx 52$ kJ.mole^{-1}, Table 3) agrees well with values of 40-60 kJ.mole^{-1} previously reported by others
532 (Wiechers et al., 1975; Mullin, 2001; Kazmierczak et al., 1982; Nancollas and Reddy, 1973;
533 Nancollas, 1979; Nancollas and Reddy, 1971).
534
535 Magnesium impurity showed a significant effect on calcite precipitation rates (Table 2). The
536 presence or absence of magnesium impurity also significantly altered the power law exponent

for the effect of supersaturation on precipitation rates (Table 3). However, the influence of magnesium was much weaker than supersaturation, the concentration of mineral phase and temperature. Accordingly, correction of precipitation kinetics with dedicated inhibition-style terms such as Eq. (11) may be considered as optional, and may depend on the level of model application. Three basic levels of application can be considered:

i. Mainly equilibrium driven – dilute systems (e.g., main line). Aqueous phase via algebraic equation set and precipitation kinetics with a high k_{cryst} without corrections for temperature and impurities.

ii. Higher wastewater strengths – e.g., digesters. Aqueous phase via algebraic equation set and precipitation kinetics with an order of magnitude estimate of k_{cryst} based on prior knowledge. Furthermore the model should at least implement kinetic temperature correction of k_{cryst}.

iii. Mission critical modelling (e.g., crystallisers, scaling, mechanistic studies). Aqueous phase via algebraic equation set, precipitation kinetics with the use of reliable kinetic information (very important to this implementation) to estimate k_{cryst} and kinetic corrections to k_{cryst} for both temperature and impurities.

The influence of other ions in wastewater such as copper, zinc, and calcium in the case of magnesium-based minerals, may have a similar effect to that observed for magnesium in the present study. It would be possible to include their complexation reactions in the algebraic equation set. Finally, where required for mission critical modelling, the kinetic effects of other ions can be accounted for via an inhibition-style correction of k_{cryst} such as is implemented for magnesium via Eq. (11).

5. Conclusions

562

563 Calcite precipitation could be effectively modelled in both extended pH titration experiments,
564 as well as constant composition experiments using a single-parameter rate equation that was
565 first-order in mineral solid state concentration, and *n*th order in thermodynamic
566 supersaturation (*n*=2 for calcite). This was effective both with and without seed crystal, with
567 no-seed experiments being simulated with a residual (<1 $mg.L^{-1}$) seed mass which effectively
568 replicated induction kinetics. The effect of temperature in precipitation rate kinetics could be
569 corrected for by an Arrhenius-style relationship, while competing ions (Mg^{2+}) could be
570 corrected for by a Langmuir adsorption isotherm. The pH and ionic strength of the aqueous
571 phase did not show substantial additional effects beyond those already accounted for in the
572 base model. Where the kinetic coefficient k_{cryst} is unknown, it should be preferentially
573 selected as a high value, since the model is tolerant to a high coefficient, but not a low
574 coefficient. Due to its general applicability, the use of this model is recommended for
575 generalised precipitation modelling in wastewater systems.

576

577 **Acknowledgments**

578

579 This research was supported financially by the University of Queensland through the UQ
580 International Scholarships (UQI) and UQ Collaboration and Industry Engagement Fund
581 (UQCIEF). Dr. Karen Steel (Chemical Engineering, UQ) is thanked for the use of the
582 chemical engineering autotitrator. Mr. Chris Carney is acknowledged for his invaluable
583 assistance with the experimental setup. Dr. Beatrice Keller-Lehmann (AWMC, UQ) and Mr.
584 Nathan Clayton (AWMC) performed analyses of water samples. Dr Flores-Alsina
585 acknowledges the People Program (Marie Curie Actions) of the EU 7th Framework
586 Programme FP7/2007-2013 under REA agreement 329349 (PROTEUS). The International

Water Association (IWA) is acknowledged for their promotion of this collaboration through their sponsorship of the IWA Task Group on Generalized Physicochemical Modelling Framework (PCM).

REFERENCES

Allison, J.D., Brown, D.S., Novo-Gradac, K.J., 1991. MINTEQA2/PRODEFA2, a Geochemical Assessment Model for Environmental Systems: Version 3.0 User's Manual, Environmental Research Laboratory, Office of Research and Development, U.S. Environmental Protection Agency.

Barat, R., Bouzas, A., Martí, N., Ferrer, J., Seco, A., 2009. Precipitation assessment in wastewater treatment plants operated for biological nutrient removal: A case study in Murcia, Spain. Journal of Environmental Management 90(2), 850-857.

Barat, R., Montoya, T., Seco, A., Ferrer, J., 2011. Modelling biological and chemically induced precipitation of calcium phosphate in enhanced biological phosphorus removal systems. Water Research 45(12), 3744-3752.

Batstone, D.J., 2009. Towards a generalised physicochemical modelling framework. Reviews in Environmental Science and Biotechnology 8(2), 113-114.

Batstone, D.J., Keller, J., 2003. Industrial application of the IWA anaerobic digestion model No. 1 (ADM). Water Science and Technology 47(12), 199-206.

Batstone, D.J., Amerlinck, Y., Ekama, G.A., Goel, R., Grau, P., Johnson, B., Kaya, I., Steyer, J.-P., Tait, S., Takács, I., Vanrolleghem, P.A., Brouchaert, C.J., Volcke, E., 2012. Towards a generalised physicochemical modelling framework. Water Science and Technology 66(6), 1147-1161.

Batstone, D.J., Keller, J., Kalyuzhnyi, S.V., Pavlostathis, S.G., Rozzi, A., Sanders, W.T.M., Siegrist, H., Vavilin, V.A., 2002. Anaerobic digestion model no. 1, IWA Publishing, London.

Boskey, A.L., Posner, A.S., 1973. Conversion of amorphous calcium phosphate to microcrystalline hydroxyapatite. A pH-dependent, solution-mediated, solid-solid conversion. The Journal of Physical Chemistry 77(19), 2313-2317.

Chen, T., Neville, A., Yuan, M., 2006. Influence of Mg^{2+} on $CaCO_3$ formation—bulk precipitation and surface deposition. Chemical Engineering Science 61(16), 5318-5327.

Chen, Y., Cheng, J.J., Creamer, K.S., 2008. Inhibition of anaerobic digestion process: A review. Bioresource Technology 99(10), 4044-4064.

Doyle, J.D., Parsons, S.A., 2002. Struvite formation, control and recovery. Water Research 36(16), 3925-3940.

Ferguson, J.F., McCarty, P.L., 1971. Effects of carbonate and magnesium on calcium phosphate precipitation. Environmental Science & Technology 5(6), 534-540.

Galbraith, S.C., Schneider, P.A., Flood, A.E., 2014. Model-driven experimental evaluation of struvite nucleation, growth and aggregation kinetics. Water Research 56(0), 122-132.

Gernaey, K.V., Flores-Alsina, X., Rosen, C., Benedetti, L., Jeppsson, U., 2011. Dynamic influent pollutant disturbance scenario generation using a phenomenological modelling approach. Environmental Modelling & Software 26(11), 1255-1267.

Hanhoun, M., Montastruc, L., Azzaro-Pantel, C., Biscans, B., Frèche, M., Pibouleau, L., 2011. Temperature impact assessment on struvite solubility product: A thermodynamic modeling approach. Chemical Engineering Journal 167(1), 50-58.

Harmandas, N.G., Koutsoukos, P.G., 1996. The formation of iron(II) sulfides in aqueous solutions. Journal of Crystal Growth 167(3–4), 719-724.

Henze, M., Gujer, W., Mino, T., van Loosdrecht, M., 2000. Activated sludge models ASM1, ASM2, ASM2d and ASM3, IWA Publishing, London.

Hina, A., Nancollas, G.H., 2000. Precipitation and dissolution of alkaline earth sulfates: Kinetics and surface energy. Alpers, C.N., Jambor, J.L. and Nordstrom , D.K. (eds), pp. 277-301, The Mineralogical Society of America, Washington, DC.

Inskeep, W.P., Silvertooth, J.C., 1988. Kinetics of hydroxyapatite precipitation at pH 7.4 to 8.4. Geochimica et Cosmochimica Acta 52(7), 1883-1893.

Joss, A., Baenninger, C., Foa, P., Koepke, S., Krauss, M., McArdell, C.S., Rottermann, K., Wei, Y., Zapata, A., Siegrist, H., 2011. Water reuse: >90% water yield in MBR/RO through concentrate recycling and CO_2 addition as scaling control. Water Research 45(18), 6141-6151.

Kazmierczak, T.F., Tomson, M.B., Nancollas, G.H., 1982. Crystal growth of calcium carbonate. A controlled composition kinetic study. The Journal of Physical Chemistry 86(1), 103-107.

Lin, Y.P., Singer, P.C., 2005. Effects of seed material and solution composition on calcite precipitation. Geochimica et Cosmochimica Acta 69(18), 4495-4504.

Lin, Y.P., Singer, P.C., 2009. Effect of Mg^{2+} on the kinetics of calcite crystal growth. Journal of Crystal Growth 312(1), 136-140.

Loewenthal, R.E., Kornmüller, U.R.C., van Heerden, E.P., 1995. Modelling struvite precipitation in anaerobic treatment systems. Water Science and Technology 30(12).

Maurer, M., Abramovich, D., Siegrist, H., Gujer, W., 1999. Kinetics of biologically induced phosphorus precipitation in waste-water treatment. Water Research 33(2), 484-493.

Morel, F., Morgan, J., 1972. A Numerical method for computing equilibria in aqueous chemical systems. Environmental Science & Technology 6(1), 58-67.

Mullin, J.W., 2001. Crystallization, Elsevier Butterworth-Heinemann, Oxford.

Musvoto, E.V., Wentzel, M.C., Ekama, G.A., 2000. Integrated chemical–physical processes modelling—II. simulating aeration treatment of anaerobic digester supernatants. Water Research 34(6), 1868-1880.

Nancollas, G.H., 1979. The growth of crystals in solution. Advances in Colloid and Interface Science 10(1), 215-252.

Nancollas, G.H., Reddy, M.M., 1971. The crystallization of calcium carbonate. II. Calcite growth mechanism. Journal of Colloid And Interface Science 37(4), 824-830.

Nancollas, G.H., Reddy, M.M., 1973. Crystal growth kinetics of minerals encountered in water treatment processes. Am Chem Soc Div Water Air Waste Chem Gen Pap 13(1).

Nielsen, A.E., 1984. Electrolyte crystal growth mechanisms. Journal of Crystal Growth 67(2), 289-310.

Nielsen, A.E., Toft, J.M., 1984. Electrolyte crystal growth kinetics. Journal of Crystal Growth 67(2), 278-288.

Nordstrom, D.K., Plummer, L.N., Langmuir, D., Busenberg, E., May Howard, M., Jones Blair, F., Parkhurst D.L., 1990. Chemical Modeling of Aqueous Systems II, pp. 398-413, American Chemical Society.

Ohlinger, K.N., Young, T.M., Schroeder, E.D., 1998. Predicting struvite formation in digestion. Water Research 32(12), 3607-3614.

Parkhurst, D.L., Appelo, C.A.J., 1999. User's guide to PHREEQC: a computer program for speciation, reaction-path, advective-transport, and inverse geochemical calculations, U.S. Dept. of the Interior, U.S. Geological Survey.

Plummer, L.N., Busenberg, E., 1982. The solubilities of calcite, aragonite and vaterite in CO_2-H_2O solutions between 0 and 90°C, and an evaluation of the aqueous model for the system $CaCO_3$-CO_2-H_2O. Geochimica et Cosmochimica Acta 46(6), 1011-1040.

Rahaman, M.S., Mavinic, D.S., Meikleham, A., Ellis, N., 2014. Modeling phosphorus removal and recovery from anaerobic digester supernatant through struvite crystallization in a fluidized bed reactor. Water Research 51(0), 1-10.

Reddy, M.M., Wang, K.K., 1980. Crystallization of calcium carbonate in the presence of metal ions: I. Inhibition by magnesium ion at pH 8.8 and 25°C. Journal of Crystal Growth 50(2), 470-480.

Rosen, C., Vrecko, D., Gernaey, K.V., Jeppsson, U., 2005. Implementing ADM1 for benchmark simulations in Matlab/Simulink, pp. 11-18, IWA, Lyngby, Denmark.

Serralta, J., Ferrer, J., Borrás, L. and Seco, A., 2004. An extension of ASM2d including pH calculation. Water Research 38(19), 4029-4038.

Scott, W.D., Wrigley, T.J.,Webb, K.M., 1991. A computer model of struvite solution chemistry. Talanta 38(8), 889-895.

Smith, S., Takács, I., Murthy, S., Daigger, G.T., Szabó, A., 2008. Phosphate complexation model and its implications for chemical phosphorus removal. Water Environment Research 80(5), 428-438.

Szabó, A., Takács, I., Murphy, S., Daigger, G.T., Licsko, I., Smith, S., 2008. Significance of Design and Operational Variables in Chemical Phosphorus Removal. Water Environment Research 80(5), 407-417.

Tait, S., Clarke, W.P., Keller, J., Batstone, D.J., 2009. Removal of sulfate from high-strength wastewater by crystallisation. Water Research 43(3), 762-772.

Tomson, M.B., Nancollas, G.H., 1978. Mineralization Kinetics: A Constant Composition Approach. Science 200(4345), 1059-1060.

van Langerak, E.P.A., Beekmans, M.M.H., Beun, J.J., Hamelers, H.V.M., Lettinga, G., 1999. Influence of phosphate and iron on the extent of calcium carbonate precipitation during anaerobic digestion. Journal of Chemical Technology & Biotechnology 74(11), 1030-1036.

van Langerak, E.P.A., Ramaekers, H., Wiechers, J., Veeken, A.H.M., Hamelers, H.V.M., Lettinga, G., 2000. Impact of location of $CaCO_3$ precipitation on the development of intact anaerobic sludge. Water Research 34(2), 437-446.

711 van Rensburg, P., Musvoto, E.V., Wentzel, M.C., Ekama, G.A., 2003. Modelling multiple
712 mineral precipitation in anaerobic digester liquor. Water Research 37(13), 3087-3097.

713 Wiechers, H.N.S., Sturrock, P., Marais, G.v.R., 1975. Calcium carbonate crystallization
714 kinetics. Water Research 9(9), 835-845.

715 Wrigley, T.J., Scott, W.D., Webb, K.M., 1992. An improved computer model of struvite
716 solution chemistry. Talanta 39(12), 1597-1603.

717

718

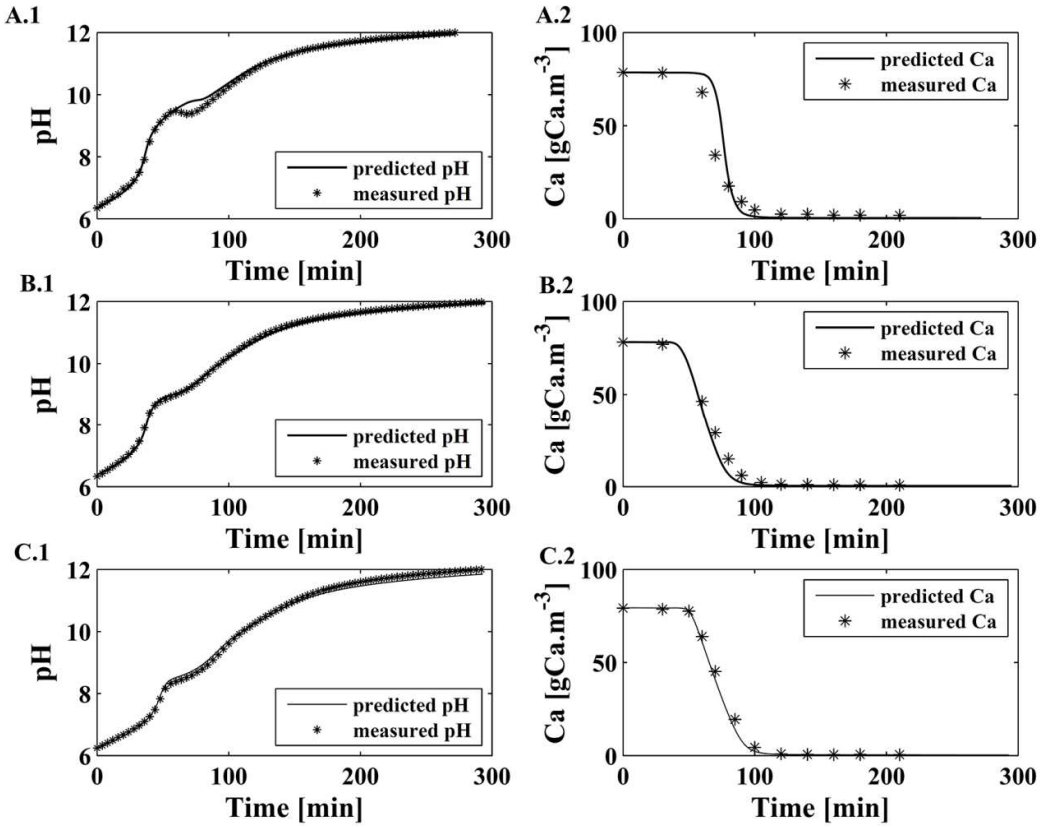

719

720

721 **Fig. 1 - Data from three titration tests with calcite precipitation (A (0mg.L^{-1} of calcite**

722 **seed), B (50mg.L^{-1} of calcite seed) and C (100mg.L^{-1} of calcite seed)) for which a model**

723 **fit of Eq. (7) gave $k_{calcite}$ = 0.0025 min^{-1}. The lines show the model fit of Eq. (7).**

724

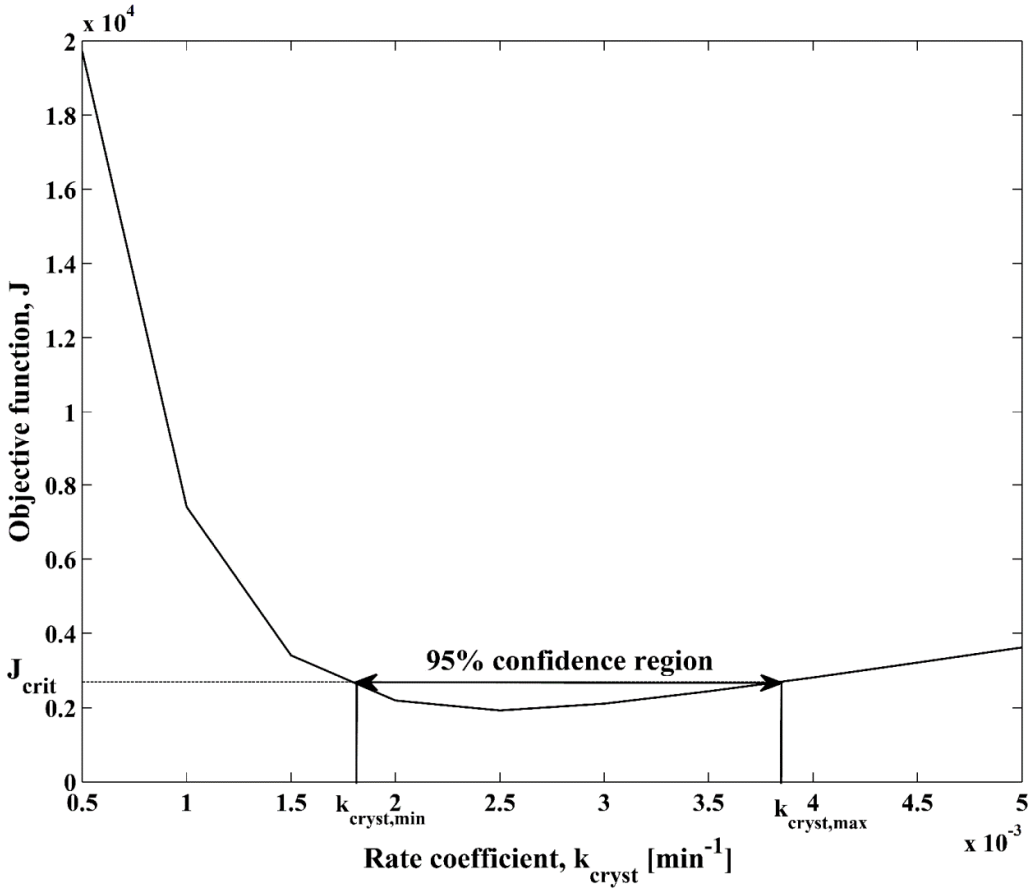

725

726 **Fig. 2 – Objective function (residual sum of squares) for the kinetic rate coefficient k_{cryst}**

727 **from the parameter estimation on the dynamic titration test data. The optimum k_{cryst}**

728 **was observed to be 0.0025 min^{-1}.**

729

730

731

732

733

734

735

736

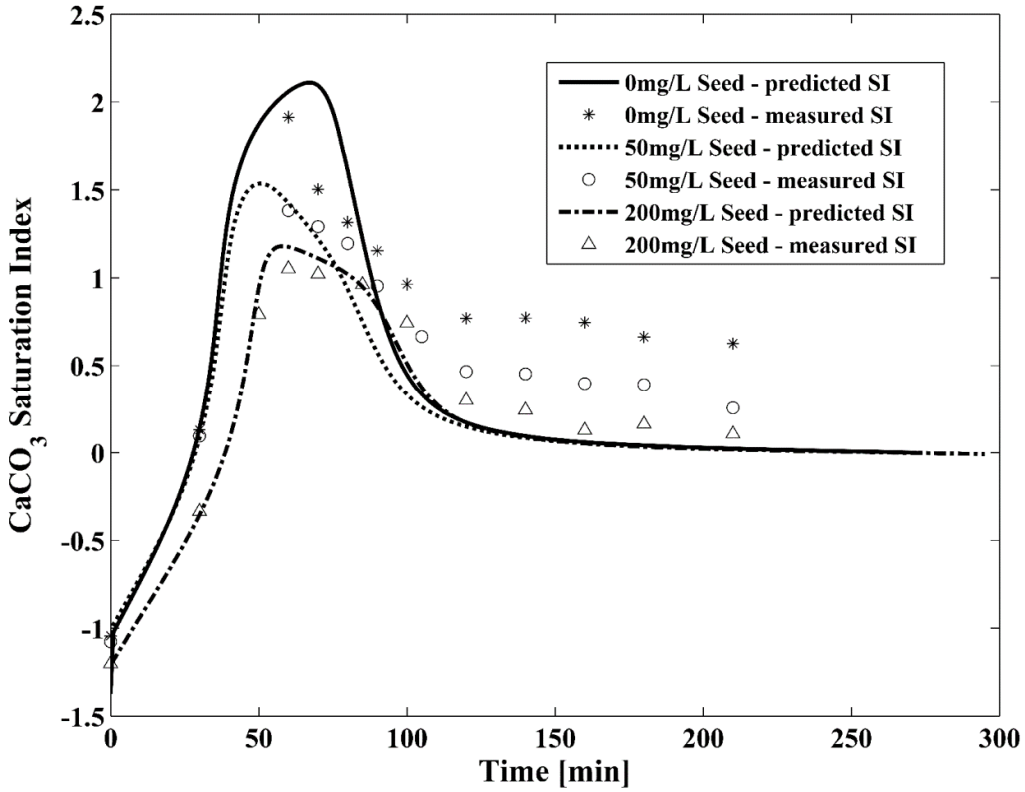

737

738 **Fig. 3 – Saturation index (*SI*) values which were calculated (from experimental**
739 **composition measurements) and simulated (k_{cryst} = 0.0025 min^{-1}) for the dynamic**
740 **titration tests with precipitation for 0 mg.L^{-1} added calcite seed (stars, solid lines), 50**
741 **mg.L^{-1} added calcite seed (circles, dashed lines) and 200 mg.L^{-1} added calcite seed**
742 **(diamonds, dot-dash lines).**

743

744

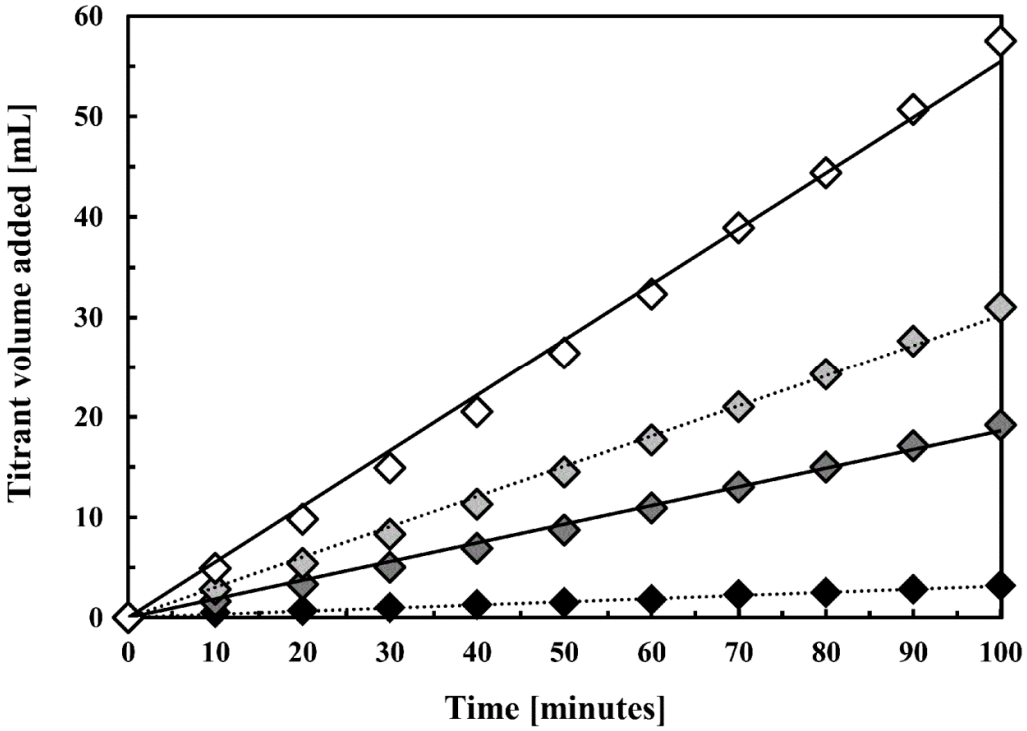

745

746 **Fig. 4 – Typical titrant volume data from the Constant Composition Experiments at a**
747 **solution pH of 8.2 (black symbols), 8.5 (dark grey symbols), 8.7 (light grey symbols) and**
748 **8.9 (white symbols). The lines are linear regression fits from which a constant slope was**
749 **obtained for the volumetric rate of titrant added (q_t for Eq. (1)).**

750

751

752

753

754

755

756

757

758

759

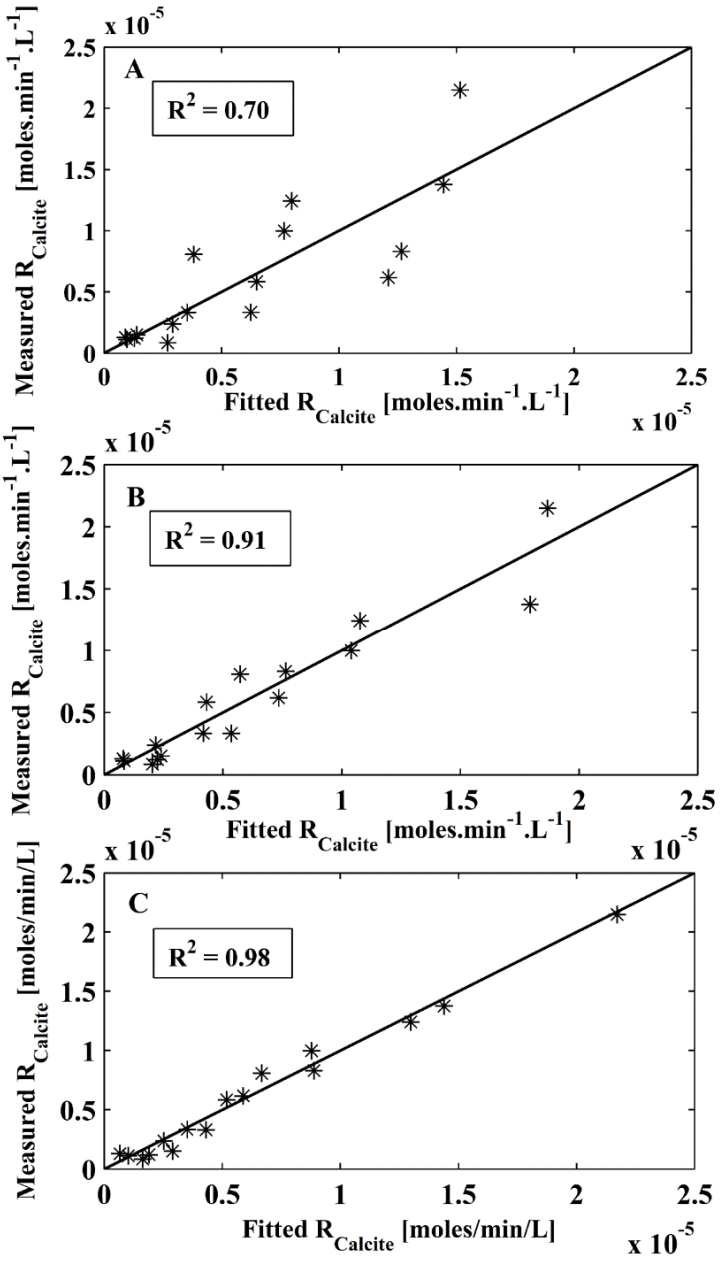

760

761 **Fig. 5 – Comparison of measured and fitted calcite precipitation rates: Full-factorial**
762 **design test set (A: baseline precipitation model fit (Eq. (7)); B: baseline model fit**
763 **corrected for temperature only with Eq. (12)); C: baseline model fit corrected for**
764 **temperature and adsorption with Eq. (11)). The line shown in each plot is y=1x.**

765

766

767

Table 1 – Test conditions and analyses for Constant Composition Method Experiments (CCM)

Parameter	**Test set 1 (full-factorial)[a]**	**Test set 2 (pH, Temperature and supersaturation)[b]**	**Test set 3 (Crystal seed mass and supersaturation)[c]**
Added $NaHCO_3$ (M)	0.004	0.002	0.002
Added $CaCl_2$ (M)	0.002 or 0.004	0.002	0.002
Added $MgCl_2$ (M)	0.00075 or 0.0015		
Seed surface area (m^2/g)	0.46	0.46	0.59
Added seed concentration ($mg.L^{-1}$)	525	525	25, 42, 62.5 or 78
Temperature (^oC)	15 or 30	20, 25, 30, 35, 40	25
Ionic strength (M)	0.1 or 0.2	0.1	0.01 – 0.2
pH	8.2	8-9	8.5
Relative supersaturation, σ	0.81-2.16	0.87-2.30	0.87-2.30
Number of experiments	16	30	25

[a] Full-factorial experimental design testing the effects of ionic strength, supersaturation, added magnesium (impurity) and temperature

[b] To further evaluate the effects of temperature, pH and supersaturation

[c] To further evaluate the effects of supersaturation and added seed crystal mass per Eq. (7)

768

769

770

771

772

773

774

775

776

Table 2 – ANOVA results for the analysis of environmental effects on CCM test results for CCM Tests 1 and 2 in Table 1.

Response – Measured calcite precipitation rate ($R_{calcite}$) with units of moles.L^{-1}.min^{-1}

Effect [a]	**p (Test 1, $n_1 = 16$)**	**p (Test 2, $n_2 = 30$)**
S_{Mg+2}	0.01339	-
σ	0.00005	2.20E-16
T	0.00049	2.70E-12
μ	0.82200	-
pH	-	0.0884
S_{Mg+2}* σ	0.06852	-
S_{Mg+2}*T	0.17843	-
σ*T	0.00318	0.0015
S_{Mg+2}*μ, S_{Mg+2}*pH, σ*μ, σ*pH, μ*T, μ*pH, pH*T	> 0.1	> 0.1
DOF_{resid}	5	23

[a] S_{Mg+2} – free dissolved magnesium concentration; σ – supersaturation; T – temperature (Kelvin); μ – ionic strength (M); Variable 1*Variable 2 – second order interaction effect; pH – pH of test solution

[b] All tested at 95% confidence level, p (>F); not significant (0.05 < p < 0.1); just significant (0.01 < p < 0.05); significant (0.001<p<0.01); highly significant (p<0.001)

777

778

779

780

781

782

783

784

785

Table 3 – Model parameter estimation values for the CCM tests (±95% confidence intervals)

Fitted parameters	CCM1 - Full-factorial design experiment	CCM2 - Test of effects of supersaturation, temperature and pH	CCM3 – Crystal seed mass and supersaturation
Supersaturation exponent, n dimensionless	2.05(±0.29)	1.3(±0.17)	1.6(±0.2)
$X_{CaCO_{3(s)}}$ exponent, y dimensionless	-	-	0.96(±0.2)
Activation energy, $E_{a,}$ kJ.mole^{-1}	52.7(±11.8)	51.68 (±7.9)	-
Adsorption coefficient, K_{ads} L.moles^{-1}	1,829(±1,473)	-	-
$k_{cryst,25C\ ,}$ min^{-1}	0.0043(±0.0013)	0.0017(±0.0002)	0.0014(±0.0011)

786

787

788

789

790

791

792

793